Computational Evaluation of the Impact of Friction Coefficient on Self-Expanding Stent and Peripheral Artery During Contact

F. Nematzadeh*

Department of Materials Engineering, Faculty of Engineering, Arak University.
Received: 29 May 2018 - Accepted: 07 July 2018

Abstract

Cardiovascular diseases (CAD) are famous as some of the chief causes of death nearby the world. In addition, peripheral artery disease (PAD) is the most known CAD. Peripheral artery stenting (PAS) is an effective substitute to peripheral endarterectomy. Self-expanding stent can be employed for minimizing the problems of interaction between PAD and stent. With the aim of evaluate biomechanical properties of Self-expanding stent and their interactions with peripheral artery, a finite element method (FEM) model was made-up which was composed of a PA and a Self-expanding stent. In the present paper, the effects of friction coefficient on the interaction between Nitinol stent and peripheral artery were studied. It was found that the increase in the friction coefficient between the Nitinol stent and peripheral artery did not result in any significant changes in the amount of stress and strain. This FEM model can provide a convenient way for evaluating biomechanical properties of peripheral stents given the effects of friction coefficient.

Keywords: Computational Evaluation, Friction Coefficient, Self-Expanding Stent, Peripheral Artery, Contact.

1. Introduction

Cardiovascular diseases (CAD) are known as some of the main causes of death around the world. Furthermore, peripheral artery disease (PAD) is the most knownCAD [1-3]. PAD is dependent on atherothrombotic syndrome associated to with high mortality of cardiovascular and cerebrovascular ischemic events [4]. PAD includes the diseases of the carotid arteries, the upper extremity arteries and superficial peripheral artery. It is a progressive disease with a variable prevalence depending on the method of diagnosis, age, sex, race and the geographic area [5]. Stent situation has been one of the chief treatments for these diseases in the last decade. Use of the stent has two main goals: short duration effect which avoids the effects of intimal dissection and the elastic recoil and long duration effect which avoids restenosis owing to the neointimal hyperplasia. Additionally, other advantages of the applications of stents can be summarized as follows: effective contour-ability to achieve an adequate fixation to the duct's wall; satisfactory resistance against the elastic recoil; resistance to fatigue due to the pulsatile flow and body's kinematics; high minimization of the size of the device to facilitate the percutaneous procedure; low thrombogenicity; and high biocompability [6]. Stent implantation has been regarded as a main approach to solve cardiovascular diseases such as peripheral artery diseases in the last decade. Recently, the application of Nitinol superelastic stents has taken the interests since they minimize such problems as restenosis after stent implantation and inflammatory artery scars in the interaction between the stent and artery [7-8].

There are many publications about the interaction between stainless steel stent and arteries. On the other hand, there are limited publications about the contact between Nitinol stent and arteries [9-14]. Migliavacca et al. [11] Compared biomechanical and clinical behavior of the stainless steel stent and the Nitinol stent for coronary artery Farnoush et al. [15] Designed braiding Nitinol stent for cardiovascular and evaluated the interaction between Nitinol stent and coronary artery. Wu et al. [16] Studied the effects of two stent designs on the interactions between Nitinol stent and carotid artery by FEM. Auricchio et al. [17] studied the mechanical behavior of two different superelastic Nitinol stent designs and their relative impact on the artery by FEM. Early et al. [18] examined the effects of two separate but related factors on stenting in peripheral arteries and coronary arteries by FEM. Auricchio et al. [19] investigated the performance of three self-expanding stent designs by FEM in a patient-specific carotid (CA) model based on computed angiography tomography (CTA) images. Senf et al. [20. Studied the influence of stent graft oversizing on radial forces in view of nitinol wire performance and vessel physical characteristics. Iannaccone et al. [21] a parametric study done for damage calculation with attention the effect of vascular structure on carotid artery stenting. Auricchio et al. [22] presented a methodology based on a global computational approach for the

*Corresponding author
Email address:f-nematzadeh@araku.ac.ir

numerical fatigue-life assessment of cardiovascular balloon expandable stents. Debusschere et al. [23] investigated an implicit FE Analysis (FEA) to model degradation of biodegradable metal stents. Cabrera et al. [24] presented combines experimental and FE Analysis (FEA) to evaluate the radial and hoop force performance of a self-expandable stents for tissue engineered heart valve implantation. Alaimo et al. [25] proposed multi-objective Genetic Algorithm (MOGA) based on Kriging response surfaces optimization framework aiming at increasing the fatigue life reducing the maximum strut strain along the structure through a local modification of the strut profile. Maleckis et al. [26] Performed comprehensive of femoropopliteal (FPA) artery stents during flexion of the limb under axial and radial compression, axial tension, bending, and torsion deformations. Conti et al. [27] proposed a methodology based on finite element analysis (FEA) able to elucidate the failure mechanisms of peripheral stents due to medical image analysis the patient-specific popliteal kinematics during leg flexion load settings. Fu et al. [28] numerically investigated how geometrical parameters (braiding angle, number and diameter of metal wires, and friction coefficients between the wires) of braided stents used for the treatment of cerebral aneurysms influence their radial compression and bending characteristics. Taggart et al. [29] studied effects of different stent design on limb flexion-induced of femoropopliteal (FPA) Artery Deformation. The objective of the present study was to use finite element method to evaluate the effect of friction coefficient on the peripheral artery behavior during contact with Nitinol wire stent.

2. Materials and Methods

2.1. Modeling and Methods/Geometry

2.1.1. Artery Geometry

The geometrical model of peripheral artery was generated by Catia (computer aided three-dimensional interactive application) and was transformed into finite element analysis code ABAQUS for the analysis. The peripheral artery was modeled as a cylinder with a length of 15 mm, internal diameter of 8 mm and thickness of 1 mm. The mesh parameters of peripheral artery are listed in Table. 1.

Table. 1. Mesh parameters for peripheral artery.

Material	Element Type	Number of Elements	Number of Nodes
Peripheral artery	C3D8H	364	840

2.1.2. Stent Geometry

The geometrical model of stent was generated by Catia and transformed into finite element analysis code ABAQUS for analysis. The stent was modeled so as to have a length of 15 mm, internal diameter of 10 mm, segmental length of 7.25 mm, radius of curvature of 2.85 mm and a wire diameter of 0.5 mm. Also, the cylinder contracting surface (crimper) was modeled so as to have a length of 20 mm and internal diameter of 10 mm. The model of stent is shown in Fig. 1. The mesh parameters of the crimper and stent are presented in Table. 2.

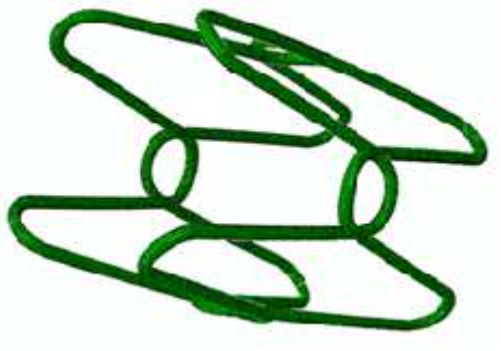

Fig. 1. Geometric model of the stent.

Table. 2. Mesh parameters for stent and crimper.

Material	Element Type	Number of Elements	Number of Nodes
Stent	C3D8I	49920	64124
Crimper	SFM3D4	3458	3549

2.2. Materials Models

2. 2.1. Artery Material Models

Polynomial form, the general polynomial form of the strain energy density function according to the strain invariants, was needed to be used for defining hyperelastic constitutive equation. It should be noted that other formulations such as the Mooney-Rivilin or the Ogden could be considered as particular cases of the polynomial model. Given the numerous uses of Mooney-Rivilin and the Ogden hyperelastic models in the recent researches and inconsistency in the results related to those models [16, 18-19,30-32], the performances of those models were studied in the present study. The constitutive equation of a hyperelastic material is based on uni-axial and bi-axial experiments on peripheral artery.The results of experimental works on the stress-strain behavior of the peripheral artery based on Lally [30] and Holzapfel [33] models are presented in Table. 3. and Table. 4.

Table. 3. The experimental results of obtained the stress-strain behavior the peripheral artery based on Lally work [30].

Stress in peripheral artery at different Extension Ratio	1.1	1.2	1.3	1.4
Strength of Intima layer (MPa)	0.07	0.4	1	2

Table. 4. The experimental results of obtained the stress-strain behavior the peripheral artery based on Holzapfel work [33].

Stress in peripheral artery at different Extension Ratio	1.1	1.2	1.3	1.4
Strength of Intima layer (MPa)	0.045	0.2	0.4	0.8
Strength of Media layer (MPa)	0.06	0.025	0.06	0.4
Strength of Adventitia layer (MPa)	0.05	0.012	0.025	0.2

The material of the peripheral artery wall was modeled by Mooney-Rivilin hyperelastic constitutive equation which is suitable for incompressible isotropic material. The strain energy density for this material was obtained by the following Eq. (1):

$$W=C_{10}(I_1-3)+C_{01}(I_2-3)+C_{20}(I_1-3)^2+C_{11}(I_1-3)(I_2-3)+C_{30}(I_1-3)^3 \quad \text{Eq.(1)}$$

where, $I_1=\lambda^2+2\lambda^{-1}$ and $I_2=2\lambda+\lambda^{-2}$ were the first and second strain invariants for uni-axial tests, λ was the associated principal stretch and C_{10}, C_{01}, C_{20}, C_{11}, C_{30} were material constants. The hyperelastic coefficients used for modeling peripheral artery are summarized in Table. 5.

Table. 5. Hyperelastic constants to describe the peripheral arterial based on Moony-Rivilin model [18, 30].

Constant	C_{10}	C_{01}	D_1
Value(MPa)	0.01895	0.00275	0.0

2.2.2. Stent Material Models

The stent material must be identified and allocated to it. Firstly, the Nitinol model was developed by Auricchio, Taylor and Lubliner [34-36].The version of this model developed by Rebelo was used for simulation of Nitinol superelastic behavior [37-38]. This model was designed on the basis of plasticity theory and the second law of thermodynamics (Helmholtz free energy).In this model, strain is decomposed into two partsEq. (2)[37]:

$$\Delta\epsilon = \Delta\epsilon^{el} + \Delta\epsilon^{tr} \quad \text{Eq. (2)}$$

Where, $\Delta\epsilon^{el}$ is a purely linear elastic strain and $\Delta\epsilon^{tr}$ is a transformation strain. Transformation of austenite to twinned martensite is driven by the shift of shear forces, and it takes place in the stress threshold assortment of the superelastic material according to the following Eq. (3)[37]:

$$F^S \le F \le F^F \quad \text{Eq.(3)}$$

Similar approach was used for defining reverse transformation on the basis of the calculation of different stress thresholds where F was transformation potential and S and F denoted martensite transformation start and finish, respectively [39].

$$\Delta\epsilon^{tr} = a\Delta\zeta\frac{\partial F}{\partial\sigma} \quad \text{Eq. (4)}$$

$$\Delta\zeta = f(\sigma,\zeta)\Delta F \quad \text{Eq. (5)}$$

$$F = \bar{\sigma} - ptan\beta + CT \quad \text{Eq. (6)}$$

Where, a is coefficient of strain, ζ is martensite fraction, σ is the Misses stress, $\bar{\sigma}$ is the misses equivalent stress, p is pressure, β and C are material constants and T is temperature.The intensity of the transformation followed a stress potential law according to the Eq.(4) and Eq.(3). Every change in stress direction generated a martensite reorientation with negligible additional effort. Additionally, the model consisted of linear shifting of stress thresholds with temperature. Given the fact that there was a volume increase related to transformation, less stress was required to produce transformation in tension, and more in compression. This effect was modeled by linear Drucker-Prager approach for the transformation potential shown in Eq.(5) [40]. The properties of materials used in this simulation are listed in Table. 6.

Table. 6. Material properties used in simulation of peripheral artery opening by Nitinol stent. The data are based on Auricchio model [38].

Symbol	Description	Unit	value
E_A	Austenite elasticity	MPa	35877
ν_A	Austenite Poisson's ratio		0.33
E_M	Martensite elasticity	MPa	24462
ν_M	Martensite Poisson's ratio	-	0.33
ε^L	Transformation strain	-	0.055
$(\delta\sigma/\delta T)_L$	stress/temperature ratio during loading	MPa T^1	6.7
σ_L^S	Start of transformation loading	MPa	489
σ_L^E	End of transformation loading	MPa	572
T_0	Reference temperature	$^\circ C$	22
$(\delta\sigma/\delta T)_U$	stress/temperature ratio during unloading	MPa T^1	6.7
σ_U^S	Start of transformation unloading	MPa	230
σ_U^E	End of transformation unloading	MPa	147
σ_{CL}^S	Start of transformation stress in compression	MPa	-
ε_V^L	Volumetric transformation strain	-	0.055
$\varepsilon_{\max}$ %	Strain limit	-	8
A_f	Austenite finish temperature	$^\circ C$	32

They were determined for opening peripheral artery based on the Auricchio model. Comparative experimental and mathematical model of Auricchio is in a reasonable agreement with the empirical data. Consequently, the properties of the materials were defined in a subroutine which was based on the Auricchio numerical model.

2.3. Boundary Conditions

The boundary condition was applied to the stent/artery model in two steps. At the beginning of the analysis, some displacement limitations on some nodes and in suitable directions were imposed. In the crimping step, a radial displacement was applied by the cylindrical contracting surface (crimper) to the stent inside the artery.

At this step, the two points at the end of the stent and one end of the peripheral artery and crimper were fixed in the longitudinal and radial directions. The other end of the artery and crimper were only fixed in the longitudinal direction. All these limitations were applied to avoid the transfer movement or model rotation during the process, so that stent could freely have radial expansion. At the first step, internal stent surface and outer crimper surface were assumed frictionless.

A radial displacement (70% diameter reduction) was enforced to the stent by crimper and then, the stent recovered its original shape after unloading. At the second step, the crimper was eliminated from the analysis and then, the stent was attached to inner wall of the peripheral artery. The boundary conditions of the stent remained as the crimping step except that the peripheral artery was restrained from translational movement at both ends. At this step, different friction between the stent and peripheral artery was considered, while all the contacts between the crimper and other parts of the model were excluded from the analysis.

Moreover, we assumed no internal pressure on the vessel wall. To decrease calculation time and to enjoy the benefits of axis symmetry, models of peripheral artery and stent were analyzed just as 1/4 geometrical model. The stent was placed exactly in the middle of the peripheral artery because the peripheral artery bases acted as resistance against the effects of edges stress of peripheral artery.

In the present work, surface-to-surface algorithm was defined by ABAQUS. Peripheral artery was selected as master surface and the stent was selected as slave surface because the movement of peripheral artery was lower than that of stent. Using this algorithm, the influence of stent nodes on peripheral artery nodes were prevented.

3. Results and Discussion

Stent implantation in human's peripheral artery to treat arterial occlusive disease is a very complex process. Also, stent implantation shows undesirable clinical results because of complexity of peripheral artery behavior in different organs and sizes. Consequently, the distribution of stress and strains in stent implantation process are very important. Some points should be taken into account in contacts between peripheral artery and stent [18, 32, , 41]. Preferably, stresses applied on the peripheral artery from stent should be reduced. Nitinol stent must have desirable superelasticity and must never be on elastic position. Furthermore, it should be safe against fracture conditions. Average allowed strain of fracture for Nitinol alloy stents depends on experience, exact chemical composition and its mechanical characteristic [7].

The stress applied by the stent on the peripheral artery should be lower than the strength of peripheral artery layers. To this end, the constant mechanical properties of arteries are determined on the basis of the experiences of the peripheral artery hyperelastic models [18, 30-31, 33]. In the present investigation, critical points on both materials were identified. Then, a change in stress, strain and displacement on peripheral artery was investigated.

The distribution of the maximum stress, the maximum strain and the maximum radial displacement on the peripheral artery wall in different friction coefficients during interaction between Nitinol stent and peripheral artery are presented. According to Fig. 2.a, Fig. 2.b, Fig. 2.c and Table.7., the increase in the friction coefficient from 0.05 to 0.10 and then, to 0.15 results in a significant reduction in the maximum stress from 0.03821 MPa to 0.03683 MPa and then, to 0.03476 MPa. The reduction ratio is about 3.61%, 5.62% and 9%, respectively. According to Fig. 3.a, Fig. 3.b, Fig. 3.c and Table. **7.**, Maximum strain decreases from 0.2460 to 0.2436 and then, to 0.2431 under the similar conditions. The reduction ratio is about 0.97, 0.2 and 1.17%, respectively. Given the applied 70% crimping on the Nitinol stent, according to Table.7., the radial displacements of arteries were almost equal.

The comparison between the maximum stress distributions on peripheral artery in interaction with Nitinol stent, According to Fig. 2.a, Fig. 2.b, Fig. 2.c and Table.7., showed the loss of stress level (6.07%) with the increase in friction coefficient. The comparison between the maximum strain distributions on peripheral artery in interaction with Nitinol stent, According to Fig. 3.a, Fig. 3.b, Fig. 3.c and Table.7., showed the loss of strain level (0.78%) with the increase in friction coefficient. Most recent studies have neglected the friction between peripheral artery and Nitinol stent [32].

However, some new researches assumed coefficient of friction as to be 0.05 [16, 19].

According to the results, insignificant change in the amount of stress and strain with the increase in friction coefficient between the Nitinol stent and peripheral artery was observed. Moreover,

according to Table. 3. and Table. 4. given the stress and strain levels on arteries, peripheral arteries were safe with high accuracy (the safety factors based on Lally and Holzapfel work is about 20, and 8, respectively) in mechanical sense.

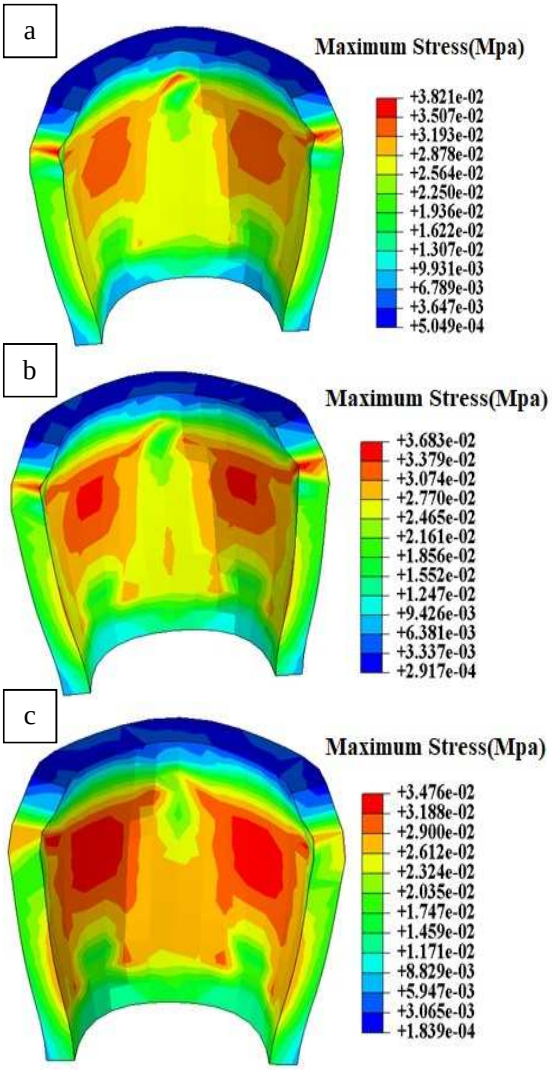

Fig. 2. Distribution Maximum Stress on peripheral artery after stent implantation (a) friction coefficient=0.05, (b) friction coefficient=0.1, (c) friction coefficient =0.15.

Table. 7. Results of the maximum stress and strain on the peripheral artery wall in different friction coefficients.

Friction Coefficient	0.05	0.1	0.15
Maximum Stress(MPa)	0.03821	0.03683	0.03476
Maximum Strain	0.2460	0.2436	0.2431

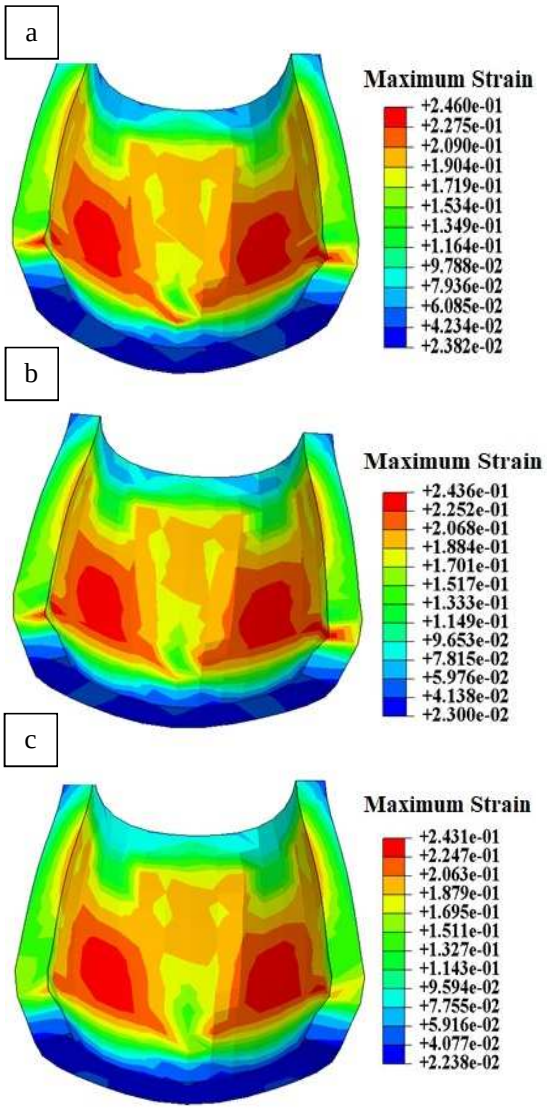

Fig. 3. Distribution Maximum Strain on peripheral artery after stent implantation (a) friction coefficient=0.05, (b) friction coefficient=0.1, (c) friction coefficient=0.15.

3.3. Limitations

In the present study, the effects of different friction coefficients on the contacts between peripheral artery and Nitinol wire stent were examined. It was believed that the results of the study were valid owing to its comparative nature. Anisotropic hyperelastic model was adopted for the artery as proposed by Lally [30] and Holzapfel [33].Also, the material parameters were calibrated on the basis of the experimental data on human peripheral artery. This model was appropriate for the purpose of the present study because it had been successfully used for similar numerical analyses that based on accurate uni-axial and bi-axial tests on several artery samples.

Moreover, although some studies have already provided experimental data on human peripheral artery, these data were used for further developments addressing anisotropic mechanical response for peripheral artery [16, 18-19, 31-32].
These simulations were much more complex owing to the contact conditions, non-linear geometries and the material nonlinearity, large deformations, buckling and bending of the stent and artery. Moreover, more experiments and simulations are needed to solve problems of contacts between peripheral artery and the Nitinol stent with respect to non-linear geometries, non-linear properties of the material, the large deformation, blood pressure, friction, plaque, and residual stresses in blood pressure.
Other limitations in this work included withdrawal of self-contact stresses of Nitinol stent segments because of their superelastic behavior, failure to consider the type and gender, plaque formation between arteries, stenosis degree of arteries, the curvature of peripheral artery, clinical work, and complex conditions of mechanical loading on the peripheral artery.

4. Conclusions

1. In the present study, a change in stress, strain and radial displacement of peripheral artery during contact with Nitinol stent were studied given friction coefficients.
2. The comparison of the results relevant to the maximum stresses and strain distribution on the peripheral artery in different friction coefficient revealed that stress level (6.07%) and strain level (0.78%) in peripheral artery were decreased with the increase in friction coefficient.
3. In total, with the increase in friction coefficient, insignificant changes were observed in the amount of stresses and strain of peripheral artery.
4. Moreover, because of stent stiffness compared to peripheral artery and owing to the curvature of peripheral artery, naturally, Stent tended to make a straight line on the peripheral artery.
5. It resulted in the occurrence of maximum stresses in contacting point of edges of stent with peripheral artery.

Acknowledgments

The author would like to thank Amir R. Khoei, Ph.D., Professor at Civil Engineering Department, Sharif University of Technology, and Dr. M. Alizadeh, professor at Mechanical Engineering Department, Iran University of Technology as well as Mr. Haghighat, research assistant at McMaster University and Mr. Madani for assisting the implementation of simulation program to modeled samples.

References

[1] S. A. Spinler, Pharmacotherapy. 26(2006), 209S.
[2] W. Rosamond, K. Flegal and G. Friday, Circulation. 15 (2007), 69.
[3] L. Norgren, W. R. Hiatt, J. A. Dormandy, M. R. Nehler, K. A. Harris and F. G. Fowkes, J. Vasc. Surg., (2007), S5A.
[4] M. H. Criqui, R. D. Langer, A. Fronk, H. S. Feigelson, M. R. Klauber, T. J. McCann, D. Browner, N. Eng. J. Med., 326 (6) (1992), 381.
[5] A. T. Hirsch, M. H. Criqui, D. Treat-Jacobson, J. G. Regensteiner, M. A. Creager, J. W. Olin, S. H. Krook, D. B. Hunninghake, A. J. Comerota, M. E. Walsh, M. M. McDermott, W. R. Hiatt, Jama. 286 (11) (2001), 1317.
[6] J. J. Belch, E. J. Topol, G. Agnelli, M. Bertrand, R. M. Califf, D. L. Clement, M. A. Creager, J. D. Easton, J. R. Gavin, P. Greenland,G. Hankey, P. Hanrath, A. T. Hirsch, J. Meyer, S. C. Smith, F. Sullivan, M. A. Weber, Arch. Inter. Med. 163 (8) (2003), 884.
[7] M. Santillo, Fracture and crack propagation study of a Superficial Femoral Artery Nitinol stent, Ms. Thesis, Pavia University, Pavia, Italy (2008).
[8] H. S. Shin, K. Park, J. H. Kim, J. J. Kim, D. K. Han, M. W. Moon, J. Bio. Comp. Poly., 24 (2009), 316.
[9] S. N. D. Chua, B. J. Mac Donald, M. S. J. Hashmi, J. Mater. Process. Technol., 155–156(2004), 1764.
[10] S. N. D. Chua, B. J. Mac Donald, M. S. J. Hashmi, J. Mater. Process. Technol., 155–56(2004), 1772.
[11] F. Migliavacca, L. Petrini, P. Massarotti, S. Schievano, F. Auricchio, G. Dubini, Biomech. Model. Mechanobiology, 2 (4)(2004), 205.
[12] W. Walke, Z. Paszenda, J. Filipiak, J. Mater. Process. Technol., 164–165(2005), 1263.
[13] V. Dehlaghi, M. Tafazoli Shadpoor, S. Najarian, J. Mater. Process. Technol., 197(2008), 174.
[14] N. Muhammad, D. J. Whitehead, A. Boor and L. Li, J. Mater. Process. Technol., 210 (2010), 2261.
[15] A. Farnoush, Q. Li, 5thAustralasian Congress on Applied Mechanics(ACAM), Brisbane, Australia,(2007), 1.
[16] W. Wu, M. Qi, X. Liu, D. Yang, W. Wang, J. Biomech,40 (13)(2007), 3034.
[17] F. Auricchio, M. Conti, S. Morganti, Levin, C. Gebeshuber, Comp. Model. Engrg. Sci., 57 (3),(2010), 225.
[18] M. Early, C. Lally, P. J. Prendergast, C. J. Boyle, A. B. Lennon, D. J. Kelly, Comp. Meth. Biome. Biomed. Engrg. 12(2009), 25.
[19] F. Auricchio, M. Conti, M. Beule,. Med. Eng. Phys., 33 (2011), 281.
[20] B. Senf, S. von Sachsen, R. Neugebauer, W.-G. Drossel, Med. Eng. Phys., 36(11)(2014),1480.

[21] F. Iannaccone, N. Debusschere, S. DeBock, M. DeBeule, J. Biomech., 47(4) (2014), 890.
[22] F. Auricchio, A. Constantinescu, M. Conti, G. Scalet, Int. J. Fatigue, 75 (2015), 69.
[23] N. Debusschere, P. Segers, P. Dubruel, Ann Biomed Eng., 44(2) (2016), 382.
[24] M. Cabrera, W. J. Oomens and T. Baaijens, J. Mech. Behav. Biomed. Mater., 68 (2017), 252.
[25] G. Alaimo, F. Auricchio, M. Conti and M. Zingales, Med. Eng. Phys., 47 (2017), 13.
[26] K. Maleckis, P. Deegan, W. Poulson, C. Sievers, J. Mech. Behav. Biomed. Mater., 75 (2017), 160.
[27] M. Conti. M. Marconi, G. Campanile. A. Reali, Meccanica, 52(3) (2017), 633.
[28] W. Fu, Q. Xia, R. Yan and A. Qiao, Bio-Med. Mater. Eng., 29 (2018), 81.
[29] M. Taggart, W. Poulson, A. Seas, P. Deegan, C. Lomneth, A. Desyatova, K. Maleckis, A. Kamenskiy, Ann. Surg. (2018), Mar, 23.
[30] C. Lally, F. Dolan, P. J. Prendergast, J. Biomech., 38(8) (2005), 1574.
[31] N. Rebelo, R. Fu, M. Lawrenchuk, J. Mater. Eng. Perf., 18 (2009), 655.
[32] H. Zahedmanesh and C. Lally, Med. Biolog. Eng. Comp., 47(2009), 385.
[33] G. A. Holzapfel, M. Stadler, T. C. Gasser, J Biomech. Eng., 127(1) (2005),166.
[34] J. Lubliner and F. Auricchio, Int. J. Solid. Struct., 33(1996), 991.
[35] F. Auricchio and R. Taylor, Compu. Meth. Appl. Mech. Eng., 143(1996), 175
[36] F. Auricchio and R. L. Taylor, Compu. Meth. Appl. Mech. Eng., 143 (1-2) (1997), 175.
[37] N. Rebelo; N. Walker and H. Foadian, In: Abaqus user's conference, Maastricht, The Netherlands, 143(2001), 421.
[38] M. Conti; M. D. Beule; P. Mortier; D. V. Loo; P. Verdonck; F. Vermassen; P. Segers; F. Auricchio and B. Verhegghe, , J. Mater. Eng. Perf., 18(2009), 787.
[39] F. Auricchio; A. Coda; A. Reali and M. Urbano, J. Mater. Eng. Perf., 18(2009), 649.
[40] J. Arghavani; F. Auricchio; R. Naghdabadi and S. Sohrabpour, Inter. J. Plasticity, 26(2010), 976.
[41] C. Henry, W. Kevin, N. Cho, Excerpt from the Proceedings of the COMSOL Conference Boston, USA (2009), 1.